Physics Letters B 664 (2008) 157–161

Contents lists available at ScienceDirect

Physics Letters B

www.elsevier.com/locate/physletb

On the magnitude of the ^{8}Li + ^{4}He → ^{11}B + n reaction cross section at the Big-Bang temperature

M. La Cognata [a], A. Del Zoppo [a,*], P. Figuera [a], A. Musumarra [a,b], R. Alba [a], S. Cherubini [a,b], N. Colonna [e], L. Cosentino [a], V. Crucillà [a,b], A. Di Pietro [a], M. Gulino [a,b], L. Lamia [a], M.G. Pellegriti [a,d], R.G. Pizzone [a], S.M.R. Puglia [a,b], G.G. Rapisarda [a,b], C. Rolfs [c,1], S. Romano [a,b], M.L. Sergi [a,b], C. Spitaleri [a,b], S. Tudisco [a], A. Tumino [a,b]

[a] *INFN-Laboratori Nazionali del Sud, Via S. Sofia 62, I95123 Catania, Italy*
[b] *Dipartimento di Metodologie Fisiche e Chimiche per l'Ingegneria, Università di Catania, I95123 Catania, Italy*
[c] *Institut für Physik mit Ionenstrahlen, Ruhr-Universität Bochum, Bochum, Germany*
[d] *Dipartimento di Fisica e Astronomia, Università di Catania, I95123 Catania, Italy*
[e] *INFN-Sezione di Bari, Via Orabona 4, I70126 Bari, Italy*

ARTICLE INFO

Article history:
Received 16 January 2008
Received in revised form 19 April 2008
Accepted 9 May 2008
Available online 16 May 2008
Editor: V. Metag

PACS:
25.10.+s
25.60.-t
26.30.+k

Keywords:
Nuclear astrophysics
Nucleosynthesis
Radioactive ion beams
Neutron detection

ABSTRACT

The ^{8}Li + ^{4}He → ^{11}B + n reaction at $E_{cm} < 2$ MeV is a process of relevant astrophysical interest for which a remarkable experimental discrepancy between inclusive and exclusive cross-section measurements exists. In this Letter, a new inclusive neutron measurement at $E_{cm} = 1.05 \pm 0.16$ MeV is given. The radioactive ^{8}Li beam was delivered by the EXCYT facility. The cross section was determined by a low-background measurement of the time correlation between the ^{8}Li projectile arrival to the target and the following neutron capture in a threshold-less 4π thermalization counter. This new data strengthens the reliability of the previous inclusive reaction cross-section data and altogether are consistent with a significant population of ^{11}B levels at high excitation energy.

Recently, in addition to other nuclear physics motivations, the availability of radioactive ion beams has given a substantial boost to the experimental study of nuclear processes which possibly occurred or that still occur at several astrophysical sites. In this work we consider the ^{8}Li + ^{4}He → ^{11}B + n reaction inside the Gamow energy region, namely at the centre of mass energy $E_{cm} < 2$ MeV.

This reaction could have made it possible to extend the primordial nucleosynthesis beyond the $A = 8$ mass gap, a hot debated issue on the early Universe evolution. In fact, observations of high-redshift, primitive astrophysical objects (quasars, galaxies, …) have shown evidence of the presence of a non-negligible abundance of heavy elements. The standard Big Bang scenario cannot allow to overcome the $A = 8$ mass gap. On the other hand, according to the inhomogeneous Big-Bang model, soon after the QGP-to-hadron transition, neutron-rich regions formed where heavy element production could have taken place. In particular, $A > 8$ nuclei should have been produced primarily following the ^{1}H(n, γ)^{2}H(n, γ)^{3}H(^{2}H, n)^{4}He(^{3}H, γ)^{7}Li(n, γ)^{8}Li(^{4}He, n)^{11}B(n, γ)^{12}B(β)^{12}C… reaction chain, despite the short ^{8}Li half life ($t_{1/2} =$ 840 ms) [1].

The ^{8}Li + ^{4}He → ^{11}B + n reaction could also play an important role in the r-process nucleosynthesis occurring in type II supernovae or in binary neutron star mergers. Indeed, in the region between the nascent neutron star and the shock front, after statistical recombination of protons and neutrons, several nuclear reactions are taking place. In particular the ^{4}He(^{3}H, γ) ^{7}Li(n, γ)^{8}Li(^{4}He, n)^{11}B chain could be responsible of the formation of seed nuclei which are eventually burnt to heavier elements in fast neutron-capture reactions. Depending on the ^{8}Li + ^{4}He → ^{11}B + n reaction rate, this reaction path might become more active than the competing processes, thus resulting in a peculiar spectrum of seed nuclei [2].

As illustrated in Fig. 1, the ^{8}Li + ^{4}He → ^{11}B + n reaction proceeds through the compound nucleus ^{12}B which, at $E_{cm} < 2$ MeV and with the positive Q-value $Q_{CN} = 10.01$ MeV, is excited in the energy range 10–12 MeV. We remark that most of the proper-

* Corresponding author. Tel.: +39095542280; fax: +390957141815.
E-mail address: delzoppo@lns.infn.it (A. Del Zoppo).
[1] Supported in part by Deutsche Forschungsgemeinschaft.

0370-2693/$ – see front matter
doi:10.1016/j.physletb.2008.05.026

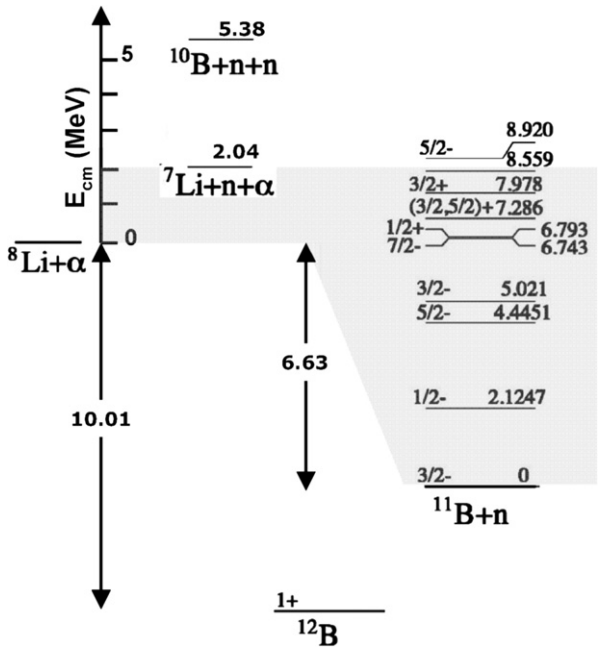

Fig. 1. Q-values and ^{11}B level scheme involved in the ^{8}Li + ^{4}He reaction at $E_{cm} < 2$ MeV.

ties of the ^{12}B levels involved in this process are unknown. The following transition to the ^{11}B + n exit channel leads to the population of one out of a maximum of nine ^{11}B levels, including the ground state (gs). The associated reaction Q-value goes from $Q_{gs} = 6.63$ MeV, for the population of the ground state, to $Q_8 = -1.93$ MeV, for the population of the level at 8.559 MeV. For the interest of nuclear astrophysics the reaction cross section summed over all ^{11}B final states is required. Its magnitude, determining the reaction rate, is of great importance because it could strengthen or weaken the veracity of the astrophysical model predictions recalled above.

Only a few experimental data on the ^{8}Li + ^{4}He → ^{11}B + n reaction cross section near the Gamow energy region exist in the literature [3–8]. Five direct studies using the radioactive projectile ^{8}Li, in which the cross section summed over the final states of ^{11}B was measured, have been reported. They can be grouped according to the detected species in: ^{11}B inclusive measurements [4,5], neutron inclusive measurement [7], ^{11}B–neutron exclusive measurements [6,8]. In the ^{11}B inclusive measurements [4,5], a 4π multiple sampling ionization chamber (MUSIC) was used as a gas target. The energy loss along the particle trajectories was measured and the detector thickness was sufficient to span the excitation function with a single beam energy. In the ^{11}B–n coincidence measurement [8], a 4π multiple sampling and tracking proportional chamber (MSTPC) was gated by the neutron signal, observed by an array of plastic-scintillators, to overcome (up to 4×10^4 s^{-1}) the very limited beam intensities supportable by the MUSIC-type detector in [4,5]. Moreover, an event by event analysis could be attempted, though a dramatic efficiency drop with decreasing energy below 2 MeV is typical of the used neutron detector and has to be taken properly into account. In the neutron inclusive measurement [7], a zero-energy-threshold 4π thermalization counter provided comparable sensitivity to all possible ^{11}B + n branches and, thanks to its characteristic capture time response, the opportunity of unambiguous reaction-neutron yield separation even in presence of an intense background level. The relatively long capture time of this technique limits the projectile rate to a few hundreds/second. But, a high statistical accuracy is not essential provided that the measurement is not affected by large systematic uncertainties.

Despite the necessarily different experimental procedures, we underline that the two complementary inclusive approaches [4,5] and [7] give comparable values of the ^{8}Li + ^{4}He → ^{11}B + n reaction cross section. The exclusive approaches [6,8] are in remarkable disagreement giving cross-section values smaller by up to a factor 4 with respect to the ones obtained in inclusive studies. Such a disagreement is so large that cannot be simply explained in terms of the presumed improved quality of the exclusive data [8].

In this Letter we present a new inclusive, low-background neutron measurement of the ^{8}Li + ^{4}He → ^{11}B + n reaction cross section at $E_{cm} \cong 1$ MeV. At this energy the discrepancy between inclusive and exclusive approaches reaches its maximum.

The experiment was performed during the commissioning of the first ^{8}Li beam delivered by the EXCYT (ISOL) radioactive ion beam facility [9] at LNS-Catania.

The ^{8}Li radioactive beam emerging from a two micro-channel plate telescope (see below) impinged onto a 4 cm ∅ and 15 cm long cylindrical gas cell filled with ^{4}He at the pressure of 150 mbar. The gas target cell was connected to the end of the beam pipe through a ∼ 5 μm (nominal thickness) Ni entrance window. This Ni window also acted as a beam energy degrader. The ^{8}Li energy was measured by a removable Si-detector placed inside the gas cell and the mean value of 3.15 MeV at approximately its centre was obtained by adjusting the energy of the delivered ^{8}Li ions to about 11 MeV. The mean energy in the centre of mass of the ^{8}Li + ^{4}He → ^{11}B + n reaction was $E_{cm} = 1.05$ MeV, with the variance square root $\Delta E_{cm} = 0.16$ MeV resulting from the propagation of the dispersions due to straggling and to the energy loss inside the target. The beam energy upper tail in the gas cell was well below the threshold of the ^{8}Li + ^{4}He → ^{7}Li + ^{4}He + n reaction (Fig. 1). In these conditions the ^{11}B + n was the only open neutron production channel of the ^{8}Li + ^{4}He reaction in this measurement.

The laboratory kinetic energy E_n of the produced neutrons varies from a few keV to approximately 10 MeV. These neutrons were detected by the Polycube 4π thermalization counter used in [10,11]. Basically, it consists of 12 cylindrical proportional counters filled with ^{3}He at the pressure of 4 bar embedded into a $40 \times 40 \times 40$ cm^3 polyethylene moderator surrounded by a 0.6 mm thick cadmium shielding and by a 4π outer layer of polyethylene approximately 12 cm thick. A 11.5 cm × 11 cm empty channel, parallel to the 12 ^{3}He counters, allowed the Polycube to enclose at its centre the gas target cell of this work. With its 4π geometry, the Polycube is capable to integrate the neutron yield over angular distributions. The dependence of the detection efficiency on the neutron energy was studied using Monte Carlo calculations, as in [10], by implementing beam pipe and gas cell in the GEANT 3.21 software replica of the whole detector used in [11]. The results obtained for mono-energetic, isotropic sources are shown in Fig. 2. It should be noted that, at low energy, the capture in the media surrounding the ^{3}He counters only causes a moderate efficiency decrease but not the onset of a threshold. Neither the electronic threshold modifies the efficiency curve versus E_n in Fig. 2, because it is smaller than the E_n-independent output spectrum of each ^{3}He counter.[2] These two characteristics make the Polycube a threshold-less detector. This is an essential feature for the aim of this work. In fact, at $E_{cm} = 1$ MeV the population of the 6th level of ^{11}B excited at 7.29 MeV is associated with a neutron energy spectrum characterised by the upper end point value of only 1 MeV. The use of a thermalization detector like Polycube is therefore fundamental

[2] A neutron capture Polycube signal has a pulse height value between 25% and 100% of the ^{3}He(n, p)^{3}H capture reaction Q-value (764 keV), the lower value corresponding to events occurring near the counter wall with the proton energy fully deposited into the housing. The electronic threshold level on each counter is typically of the order of 0.1Q.

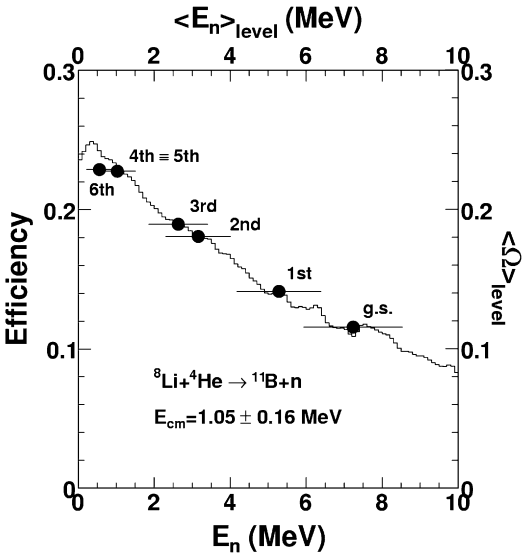

Fig. 2. Monte Carlo simulations of the neutron detector performances. The histogram represents the dependence of the detection efficiency (left vertical axis) on the incident neutron energy (bottom horizontal axis). The filled circles depict the dependence of $\langle\Omega\rangle_{\text{level}}$ (right vertical axis) on the mean incident neutron energy $\langle E_n\rangle_{\text{level}}$ (top horizontal axis) for the studied reaction case. Each horizontal bar shows the neutron energy spread (variance square root).

for minimizing systematic uncertainties related to efficiency corrections for these low-energy neutrons, which could otherwise be completely missed by detectors based on proton recoil, such as plastic scintillation counters.

Finally, the characteristic neutron capture (nc) probability density $\frac{dP_{\text{nc}}(t_{\text{capt}})}{dt_{\text{capt}}}$ of the time t_{capt} elapsed between the production of the neutron and its capture in the Polycube detector is known with good experimental accuracy. This response function was measured by using a ^{252}Cf source and the data was corroborated by Monte Carlo simulations. The measured data is very much consistent with the following superposition of two exponentially decreasing components

$$\frac{dP_{\text{nc}}}{dt_{\text{capt}}} = \frac{q}{\tau_{\text{fast}}} e^{-\frac{t_{\text{capt}}}{\tau_{\text{fast}}}} + \frac{1-q}{\tau_{\text{slow}}} e^{-\frac{t_{\text{capt}}}{\tau_{\text{slow}}}}, \tag{1}$$

characterized by different mean capture times τ_{fast} and τ_{slow} with relative intensity $q(\leqslant 1)$ and $1-q$, respectively. The form of the capture time distribution (1) follows from the presence of mainly two weakly absorbing media, polyethylene and air in the (almost empty) central channel, which determine different migration paths and lives of the thermalized neutrons before being captured in ^{3}He, the smaller the mean density along the migration path, the longer the capture time scale. The values of the parameters $\tau_{\text{fast}}, \tau_{\text{slow}}$ and q are independent of the neutron energy in the 0.1–20 MeV range. The measured parameter values are $\tau_{\text{fast}} = 68 \pm 0.4$ μs, $\tau_{\text{slow}} = 169 \pm 0.7$ μs and $q = 0.58 \pm 0.003$. The detailed description of the experiment and simulation procedures is reported in [11]. Such a feature was used here to measure the wanted cross section σ (mb) of the $^8\text{Li} + {}^4\text{He} \rightarrow {}^{11}\text{B} + \text{n}$ reaction by comparing the experimental count distribution $\frac{dN(t_{\text{capt}})}{dt_{\text{capt}}}$ with the characteristic $\frac{dP_{\text{nc}}(t_{\text{capt}})}{dt_{\text{capt}}}$, namely

$$\frac{10^{27}}{\bar{\Omega} \cdot N_{\text{proj}} \cdot D_{^4\text{He}}} \frac{dN(t_{\text{capt}})}{dt_{\text{capt}}} = \sigma \cdot \frac{dP_{\text{nc}}(t_{\text{capt}})}{dt_{\text{capt}}} + b, \tag{2}$$

where N_{proj} is the number of projectile nuclei, $D_{^4\text{He}}(\text{cm}^{-2})$ is the target thickness and b (mb μs^{-1}) denotes the possible background level. In (2) $\bar{\Omega}$ is the average value of the Polycube detection efficiency for the global $^8\text{Li} + {}^4\text{He} \rightarrow {}^{11}\text{B} + \text{n}$ reaction neutron energy spectrum, namely $\bar{\Omega} = \sum f_{\text{level}} \langle\Omega\rangle_{\text{level}}$, $\langle\Omega\rangle_{\text{level}}$ being the detection efficiency averaged over the laboratory neutron energy spectrum associated to a given ^{11}B level, f_{level} being the relative population intensity of that ^{11}B level. The set of $\langle\Omega\rangle_{\text{level}}$-values was determined by implementing the initial beam energy spread, the beam energy loss, the range of the reaction point coordinate, the relevant Q-values, the ^{11}B level scheme in Fig. 1, the reaction kinematics and isotropic neutron production in the centre of mass into the GEANT simulation code [11]. Fig. 2 shows the value of $\langle\Omega\rangle_{\text{level}}$ for each of the seven accessible levels at the considered centre of mass energy as a function of the corresponding mean neutron energy, the variances in the histories of the Monte Carlo calculation determining the statistical uncertainty of about 0.7%. Deviations from the histogram in Fig. 2, which signal an increased forward escape along the detector central channel, caused by the specific centre of mass motion, only manifest in the value of $\langle\Omega\rangle_{6\text{th}}$.

The set of f_{level}-values in a narrow interval around $E_{\text{cm}} = 1$ MeV is unknown. Consequently, uniform ^{11}B level population was assumed, the value $\bar{\Omega} = 0.195 \pm 0.0005$(statistical) was established and used in (2). It should be noted that the big concentration into 40% only of the range spanned by the $\langle\Omega\rangle_{\text{level}}$-values in Fig. 2 (five out of the seven values are between 0.18 and 0.23) sets robust constraints on the variability of $\bar{\Omega}$ with varying the f_{level}-set. Therefore, in the specific reaction case studied here, this fact tends to weaken the impact of the unknown population pattern on the systematic uncertainty level attributable to $\bar{\Omega}$. In fact, for instance, if the non-uniform f_{level} intensity values in the broad region of $E_{\text{cm}} = 0.7$–2.6 MeV [8] are considered instead, the ground and the third levels being mostly fed, the result deviates by only 3.5% from the value of $\bar{\Omega}$ which competes to the uniform pattern. This is the order of magnitude of the relative systematic uncertainty affecting $\bar{\Omega}$ for not extremely non-uniform population patterns.

A figure of merit of the measurements based on (2) is the signal to background ratio $\sigma : 2b\bar{t}_{\text{capt}}$, where b is the background level and $2\bar{t}_{\text{capt}}$ is the time interval in which the majority of the capture events occurs, $\bar{t}_{\text{capt}} = q \cdot \tau_{\text{fast}} + (1-q) \cdot \tau_{\text{slow}} = 110$ μs is the mean capture time.

The time t_{capt} in (1) and (2) was measured by a time to amplitude converter (TAC) with the time range adjusted to 330 μs, about three times the mean capture time $\bar{t}_{\text{capt}}$. The neutron production instant was identified by the arrival of the projectile to the target, which was assumed as the zero of the capture time scale. This was obtained by a 99% (intrinsic efficiency) two-microchannel plates (MCP) telescope located upstream along the beam axis as in [12]. Dark counts of the individual MCP's were discarded by the requested MCP–MCP fast coincidence within a 50 ns wide window. This device was also used for noise-free counting of the incident projectile number N_{proj}. Such a background-free time-zero reference was sent to the START input of the TAC. Before starting the experiment, the 100% purity with which the ^{8}Li beam is delivered by the ISOL facility [9] was checked to persist at near target position by placing near the second MCP a removable Si telescope for $\Delta E - E$ measurements complemented by the time of flight information using the first MCP temporarily located 5 m upstream. During the experiment the beam purity was continuously monitored by the time of the flight between the two MCPs. In the previous works [7,12] the MCP-telescope was used also to monitor beam contaminant intensities using time of flight over a 5 m path. In the present work, thanks to the excellent beam purity, a long flight path was not necessary. Therefore, with the aim of reducing significantly the neutron background rate associated with the beam production procedure, the MCP–MCP distance was shortened to 1 m, still ensuring the possibility to identify the wanted projectile. Then the ^{8}Li intensity value was adjusted so as to keep the START mean rate R as low as 200 s^{-1}. The distortions caused

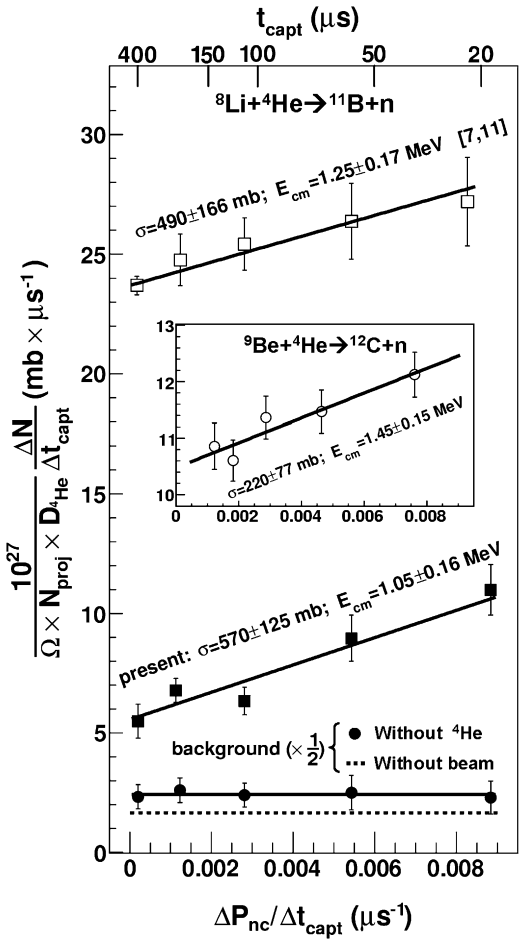

Fig. 3. Correlation plots according to (2) for the indicated reactions. The $t_{\rm capt}$ scale is shown on the top.

by the stochastic behaviour of the projectile arrival time sequence were of the order of $R \cdot \bar{t}_{\rm capt} \cong 2\%$.

The neutron capture instant was obtained by the OR of the 12 proportional counter logic outputs. This was sent to the STOP input of the TAC. The expected rate of correlated neutrons was about 0.2 events/(day mb).

Fig. 3 shows the differential count distribution $\frac{\Delta N(t_{\rm capt})}{\Delta t_{\rm capt}}$ measured in this work as a function of the Polycube capture time probability density (1) (filled squares). The data follows the linear dependence expected for correlated neutron capture according to (2). The slope of the linear best fit determines the ^{8}Li + ^{4}He → ^{11}B + n reaction cross-section value $\sigma = 570 \pm 125$(statistical) mb at $E_{\rm cm} = 1.05 \pm 0.16$ MeV. The signal to background ratio of this new measurement can be deduced from Fig. 3 to be $\approx 1:2$.

Care was paid to limit to tolerable levels possible contaminations of correlated neutron background, like that from the sub-barrier break-up into ^{7}Li + n of the weakly bound ^{8}Li when passing through the Ni window (barrier height ∼ 12 MeV) and stopping inside a thick tantalum disk (barrier height ∼ 30 MeV) at the end of the gas target cell. The ^{8}Li energy measured values behind and beyond the Ni window determined the $3.5 \leqslant E_{\rm cm} \leqslant 8.8$ MeV range in which the ^{8}Li + ^{58}Ni collisions occurred. A realistic estimate of the ^{8}Li break-up cross section versus centre of mass energy was evaluated by appropriately scaling [13] to ^{8}Li + ^{58}Ni of the total break-up/transfer data from ^{8}Li + ^{208}Pb [14] and of the break-up data from ^{9}Be + ^{197}Au [15]. The expected contamination amounts to at most 1% of the ^{8}Li + ^{4}He → ^{11}B + n cross-section value measured here. The contribution from ^{8}Li break-up on Ta ($E_{\rm cm} < 3$ MeV) is smaller by orders of magnitude. Nevertheless, to avoid misinterpretation of the origin of the correlated neutrons observed, a separate measurement was also performed without ^{4}He. The same gas target cell was filled with Xe at the pressure of 22 mbar in order to have comparable ^{8}Li energy loss, with Xe alone or with ^{4}He alone, along the path to the tantalum disk. Fig. 3 shows that, without ^{4}He, the resulting differential count distribution is constant (filled circles). This demonstrates that the ^{8}Li + ^{4}He reaction was the only significant source of correlated neutrons of this experiment. It should also be noted that, within the error bars, the value of this background measured without ^{4}He (filled circles) coincides with that of the background level b determined by the linear fit to the ^{4}He–target data points (filled squares in Fig. 3) according to (2). It is also worth mentioning that the background measured without beam (dashed line)[3] represents as much as 60% of the total background level observed in the reaction data (filled squares).

Fig. 3 also shows the $\frac{\Delta N(t_{\rm capt})}{\Delta t_{\rm capt}}$ data at $E_{\rm cm} = 1.25 \pm 0.17$ MeV (open squares) reported in [7,11] and obtained by bombarding the ^{4}He target by a secondary ^{8}Li beam produced in flight as described in [12]. The comparison evidences clearly the lower background level of the present measurement. In the present work the signal to background ratio has increased by approximately a factor 4–5 and, in particular, the background contribution associated with the beam production procedure has decreased by a factor 10. Thanks to such an enhancement in the S/N ratio, with comparable signal count statistics we could improve the accuracy on the wanted cross-section value by a factor 1.6.

Finally, we have corroborated these ^{8}Li + ^{4}He → ^{11}B + n cross-section data with a positive check of the experimental procedure adopted here. We have studied the ^{9}Be + ^{4}He → ^{12}C + n reaction at $E_{\rm cm} = 1.45 \pm 0.15$ MeV. The measured capture time correlation plot is shown in the inset of Fig. 3. A count statistics comparable to that of the measurements using ^{8}Li was considered. Within the experimental uncertainty, the slope of the linear data fit is consistent with the mean value of 187 ± 1 mb as deduced from independent high-accuracy cross-section data available in the literature for this reaction [16] in the considered energy interval. This result on the ^{9}Be + ^{4}He → ^{12}C + n reaction evidences that there are not large systematic errors which affect the experiment and data analysis procedures.

Fig. 4 summarizes the present state of the art of the ^{8}Li + ^{4}He → ^{11}B + n cross-section data. Three groups of direct measurements, in which the ^{8}Li unstable isotope was produced and used as projectile, have been performed till now. The first group (also chronologically) includes two sets of measurements, at $E_{\rm cm} \geqslant$ 1.5 MeV in [4] and at $E_{\rm cm} \geqslant 0.7$ MeV in [5], which agree on the magnitude of the cross section determined by the inclusive detection of the ^{11}B nuclei formed in the reaction. The second group comprises the measurement at $E_{\rm cm} = 1.25 \pm 0.17$ MeV in [7] and that at $E_{\rm cm} = 1.05 \pm 0.16$ MeV in this work, in which the reaction cross section has been determined by the inclusive detection of the neutron.

The third group includes the exclusive ^{11}B–neutron coincidence experiment at $E_{\rm cm} \geqslant 1.5$ MeV in [6] and that at $E_{\rm cm} > 0.7$ MeV in [8].

The magnitude of the cross section measured in this work strongly supports the reliability of the previous cross-section measurement [7,11], which used the same neutron detection approach at slightly higher centre-of-mass energy. Moreover, both previous and present inclusive neutron data points are unquestionably

[3] This background is almost exclusively due to alpha-emitter nuclides in the stainless steel housing of the ^{3}He proportional counters.

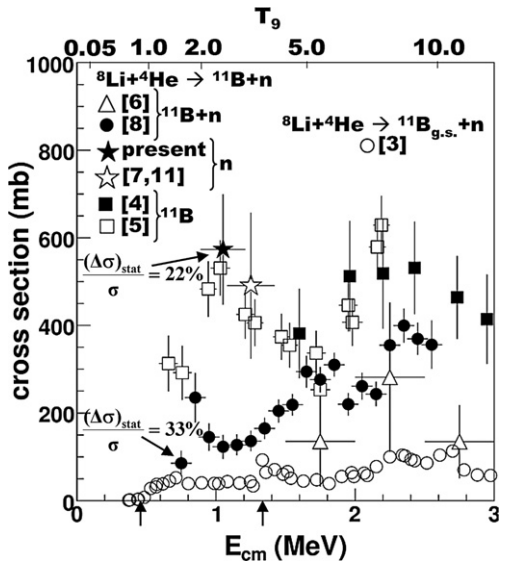

Fig. 4. ^{8}Li + ^{4}He → ^{11}B + n cross-section data measured with the three indicated experimental approaches. The ^{8}Li + ^{4}He → $^{11}B_{gs}$ + n cross section is also shown (open circles). The arrows close to the energy axis delimit the Gamow region at $T_9 = 2$. The temperature scale (in units of 10^9 K) is reported on the top.

closer to the complementary inclusive measurements [5] than to the exclusive data [8]. Therefore, the result of the present experiment enforces the symptom of a remarkable discrepancy at $E_{cm} < 1.7$ MeV between the whole ensemble of inclusive cross-section data on one side and the exclusive data [8] on the other. Unlikely this is due to an insufficient statistical accuracy and/or energy uncertainty of the inclusive data compared to that of the exclusive data (see Fig. 4). Moreover, in the inclusive approach of this work there are not so large systematic errors which might adequately justify this discrepancy. Even abandoning the uniform population hypothesis and considering just the non-uniform ^{11}B level population pattern proposed in [8], the corresponding value of $\bar{\Omega} = 0.188$ in (2) would lead to increase by a further 3.5% the total cross-section values determined in this work.

Fig. 4 also shows the ^{8}Li + ^{4}He → $^{11}B_{gs}$ + n cross-section data deduced in [3] from the inverse reaction ^{11}B(n, ^{4}He)^{8}Li. In the Gamow region these data are as much as an order of magnitude smaller than the inclusive ones, because the indirect study is sensitive to the process that leads to the ground state population of ^{11}B only. The exclusive $^{11}B_{gs}$–n data also reported in [8], with the laboratory neutron energy being of the order of several MeV, are in agreement with the results in [3]. Thus, in the comparison of Fig. 4, it seems that the ^{11}B excited level summed contribution in the exclusive measurement [8] is significantly weaker than that indicated by all inclusive measurement data. Actually, due to the neutron detection threshold,[4] the observation of reaction exit channels resulting in the population of the highest ^{11}B levels (accompanied by less energetic neutrons) might have been critical in the exclusive measurement [8]. In our analysis, if the 6th level provides the predominant contribution, the detection efficiency $\bar{\Omega}$ would approach its maximum value $\bar{\Omega}_{max} \cong \langle\Omega\rangle_{6th} \cong 0.23$ (Fig. 2) and the total cross section would decrease by at most 20%. Accordingly, a systematic uncertainty of the order of 10% should be included in the total error lower half-bar of the cross-section values determined in this work, namely $\sigma = 570^{+125}_{-140}$ mb at $E_{cm} = 1.05 \pm 0.16$ MeV and $\sigma = 490^{+166}_{-173}$ mb at $E_{cm} = 1.25 \pm 0.17$ MeV.

In conclusion, this Letter presents accurate new data on the inclusive ^{8}Li + ^{4}He → ^{11}B + n reaction cross section at $E_{cm} \cong$ 1 MeV. Since an important fraction of neutrons might be emitted with low laboratory energy, the use of a threshold-less thermalization detector has allowed to minimize systematic uncertainties related to efficiency corrections. Moreover, it is important to stress that the technique used in this work shows a significant sensitivity to all the involved laboratory neutron energies (and to the corresponding ^{11}B excited levels), thus ensuring a truly complete measurement of the reaction cross section.

The results of this work, performed with improved experimental and analysis procedures, confirm the large value of the cross section given in [7] and are in good agreement with other data obtained by inclusive ^{11}B detection [5]. Further studies are needed to solve the large discrepancy with the exclusive measurement reported in [8].

References

[1] E. Witten, Phys. Rev. D 30 (1984) 272;
J.H. Applegate, et al., Phys. Rev. D 35 (1987) 1151;
R.A. Malaney, W.A. Fowler, in: G.J. Mathew (Ed.), The Origin and Distribution of Elements, World Scientific, Singapore, 1988, p. 76;
R.A. Malaney, W.A. Fowler, Astrophys. J. 333 (1988) 14;
T. Kajino, R.N. Boyd, Astrophys. J. 359 (1990) 267;
S. Matsuura, et al., Phys. Rev. D 72 (2005) 123505, and references therein.
[2] M. Terasawa, et al., Astrophys. J. 562 (2001) 470;
T. Kajino, in: Proceedings of Nuclei in the Cosmos, vol. 7, 2002;
T. Kajino, Nucl. Phys. A 718 (2003) 295c;
T. Sasaqui, et al., Astrophys. J. 634 (2005) 534;
T. Kajino, et al., Nucl. Phys. A 704 (2002) 165c;
S. Rosswog, et al., Nucl. Phys. A 688 (2001) 344c.
[3] T. Paradellis, et al., Z. Phys. A 337 (1990) 211.
[4] R.N. Boyd, et al., Phys. Rev. Lett. 68 (1992) 1283.
[5] X. Gu, et al., Phys. Lett. B 343 (1995) 31.
[6] Y. Mizoi, et al., Phys. Rev. C 62 (2000) 065801.
[7] S. Cherubini, et al., Eur. Phys. J. A 20 (2004) 355.
[8] H. Ishiyama, et al., Phys. Lett. B 640 (2006) 82.
[9] G. Ciavola, et al., Nucl. Phys. A 701 (2002) 54c.
[10] P.R. Wrean, R.W. Kavanagh, Phys. Rev. C 62 (2000) 055805.
[11] A. Del Zoppo, et al., Nucl. Instrum. Methods A 581 (2007) 783.
[12] C. Agodi, et al., Nucl. Instrum. Methods A 565 (2006) 406.
[13] S.B. Moraes, et al., Phys. Rev. C 61 (2000) 064608, and references therein.
[14] J.J. Kolata, et al., Phys. Rev. C 65 (2002) 054616.
[15] J. Unternahrer, et al., Phys. Rev. Lett. 40 (1978) 1078.
[16] P.R. Wrean, et al., Phys. Rev. C 49 (1994) 1205.

[4] See Fig. 4 in [6] and Fig. 7 in Hashimoto et al. cited in [8] as Ref. [11].